Research paper

Prediction of dissolution time and coating thickness of sustained release formulations using Raman spectroscopy and terahertz pulsed imaging

Joshua Müller [a], Daniela Brock [a], Klaus Knop [a], J. Axel Zeitler [b], Peter Kleinebudde [a,*]

[a] Institute of Pharmaceutics and Biopharmaceutics, Heinrich-Heine-University, Duesseldorf, Germany
[b] Department of Chemical Engineering and Biotechnology, University of Cambridge, Cambridge, UK

ABSTRACT

Raman spectroscopy was implemented successfully as a non-invasive and rapid process analytical technology (PAT) tool for in-line quantitative monitoring of functional coating. Coating experiments were performed at which diprophylline tablets were coated with a sustained release formulation based on Kollicoat® SR 30 D. Using PLS a multivariate model was constructed by correlating Raman spectral data with the mean dissolution time as determined by dissolution testing and the coating thickness as measured by terahertz pulsed imaging.

By performing in-line measurements it was possible to monitor the progress of the coating process and to detect the end point of the process, where the acquired coating amount was achieved for the desired MDT or coating thickness.

© 2011 Elsevier B.V. All rights reserved.

1. Introduction

In formulation of solid dosage forms film coating represents an important unit operation. It can serve different purposes such as taste masking, product identification and protective layering. Functional coating is used to improve the therapeutic effect, for example, enteric or controlled release coatings, which influence location and period of drug release [1–3]. It is a challenging operation in terms of achieving the desired amount of coating thickness and coating uniformity. To ensure the quality of coated dosage forms it is desirable to develop a tool that is able to monitor the coating operation and detect the end point of the process.

Process analytical technologies (PATs) are commonly employed in the manufacturing processes of the pulp and paper or chemical and petroleum industries [4–6]. The US Food and Drug Administration (FDA) has redefined this concept in the pharmaceutical context and implemented it as part of an initiative to focus on improving manufacturing quality in the pharmaceutical industry. Process understanding, optimisation of manufacturing efficiency and reproducibility of product quality are the primary objectives of the guidance document with regard to process analytical technology (PAT) issued by the FDA [7]. An overview of the applications of PAT in the pharmaceutical industry is provided elsewhere in

the literature [8–10]. It impacts on all aspects from controlling the synthesis of the active pharmaceutical ingredient, identifying raw materials in processing up to determining the concentration of the API in the final dosage form [10].

Previous research showed that spectroscopic methods in combination with multivariate data analysis are a suitable technology platform for PAT applications. Due to its low cost, the availability of compact and very robust process sensors and its good sensitivity to moisture and chemical properties near-infrared spectroscopy (NIR) was established as a PAT tool for pharmaceutical applications. It is now used for end point determination in blending, process control of granulation, drying and coating operations and in many other applications [11–18].

With the development of cheaper and more rugged laser technology Raman spectroscopy has recently emerged as an alternative sensor technology for PAT applications in pharmaceutical processing [19–27].

In addition, terahertz pulsed imaging (TPI) is becoming an established technique in the pharmaceutical industry to directly measure the coating thickness and its spatial uniformity on coated tablets [28–31]. As the terahertz measurements are non-destructive and the measurements require no multivariate calibration, it is an attractive technique to analyse pharmaceutical coatings.

This study focused on the implementation of Raman spectroscopy as a non-invasive and rapid process analytical technology (PAT) tool for in-line quantitative monitoring of functional coating. To achieve this aim a multivariate calibration based on offline measurements was developed using tablets collected at different

* Corresponding author. Institute of Pharmaceutics and Biopharmaceutics, Heinrich-Heine-University, Universitaetsstrasse 1, 40225 Duesseldorf, Germany. Tel.: +49 211 811422; fax: +49 211 8114251.
E-mail address: kleinebudde@uni-duesseldorf.de (P. Kleinebudde).

process time during coating in a small-scale pan coater. Coating experiments were performed at which diprophylline tablets were coated with a sustained release formulation based on Kollicoat® SR 30 D. The Raman spectral measurements were correlated with the mean dissolution time (MDT) as determined by dissolution testing and the coating thickness as measured by TPI. The multivariate Raman model was then tested in-line by monitoring the progress of a coating process.

2. Materials and methods

2.1. Materials

2.1.1. Diprophylline cores

Biconvex diprophylline cores (4 mm in height, 8 mm in diameter, and an average weight of 200 mg) were composed of 10% (w/w) diprophylline (BASF, Ludwigshafen, Germany), 84.5% (w/w) lactose monohydrate (Flowlac® 100, Meggle, Wasserburg, Germany), 5% (w/w) copovidone (Kollidon® VA 64, BASF, Ludwigshafen, Germany) and 0.5% (w/w) magnesium stearate (Welding, Hamburg, Germany).

2.1.2. Coating dispersion

The aqueous coating dispersion contained 42% w/w polyvinyl acetate (Kollicoat® SR 30 D, BASF, Ludwigshafen, Germany), 5% w/w polyvinyl alcohol polyethylene glycol graft copolymer (Kollicoat® IR, BASF, Ludwigshafen, Germany), 0.5% w/w povidone (Kollidon® 30, BASF, Ludwigshafen, Germany), 1% w/w triacetine (Riedel-de Haën, Seelze, Germany), 0.5% w/w titanium dioxide (Evonik, Germany), 4% talcum (C.H. Erbslöh KG, Krefeld, Germany) and 47% deionised water.

2.2. Coating process

Two batches (A and B) with a batch size of 3.5 kg each were coated in a Laboratory Film Coater BFC 5 (L.B. Bohle, Ennigerloh, Germany) with a pan diameter of 316 mm and a length of 356 mm.

The process parameters are listed in Table 1. In both cases tablets were coated with 8 mg functional polymer/cm². The required quantity of polymer is related to the surface area of the tablet cores and was calculated as described in the literature [32,33].

Six samples were removed from the coating pan at 0, 37, 73, 143, 215, 253 and 287 min during the coating process for offline analysis.

In-line monitoring using Raman spectroscopy was performed throughout the process as outlined in Section 2.7.

2.3. Raman analysis

A P^hAT System (Kaiser Optical Systems, Ann Arbor, MI, USA) equipped with a noncontact optic sampling accessory was used for the Raman analysis. The excitation laser (785 nm diode laser, 14.1 mW/mm²) was directed to the sample using an optical fibre. Using a set of lenses at the probe head the laser beam was collimated to form a circular illumination area with a diameter of 6 mm (area: 28.3 mm²) to cover a large sampling area. This wide area illumination scheme reduces the errors due to focusing and

improves the reproducibility of sampling [34,35]. The backscattered radiation was collected by an array of 50 optical fibres in the probe head and delivered to the spectrometer. A holographic transmission grating was used to disperse the collected backscatter from the optical fibres, and signal integration was performed using an air-cooled CCD detector. Data collection and data transfer were automated using the HoloGRAMS™ (Kaiser Optical Systems) data collection software package, the HoloREACT™ (Kaiser Optical Systems) reaction analysis and profiling package, the Matlab® software package (version 6.5; The MathWorks, Inc., Natick, MA, USA), and Microsoft Excel®.

The samples that were collected during the film coating process were measured offline from both sides with a working distance of 22 cm and a scanning time of 15 s using the Raman probe. The measurement was followed by cosmic ray filtering and dark subtraction. The two spectra from both sides of each tablet were averaged, and the average spectrum was used for the subsequent model development.

2.4. Terahertz pulsed imaging analysis

Coating thickness analysis was performed using a TPI imaga 2000 system with a bandwidth of 0.06–3 THz (TeraView Ltd., Cambridge, UK). The entire surface of the sampled tablets was measured in full scanning mode with a point spacing of 200×200 μm using a scan range of 1 mm optical delay in air. At each measuring point a single pulse of coherent broadband terahertz radiation is focused on the sample and reflection signals are collected by a receiver unit. Reflection pulses occur at each interface, where optical attributes of the medium under investigation change while other parts of the radiation penetrate further into the tablet [31].

Coating thickness was calculated for each pixel using the time-of-flight between the reflection signals of tablet surface peak and coat-core interface peak (TPIView software, version 3.0.3, TeraView Ltd., Cambridge, UK). The time axis was transformed to a distance axis using a refractive index of 1.53. Mean coating thickness and standard deviations were calculated for both tablet sides separately.

2.5. Dissolution testing

Dissolution testing was carried out using the same tablets that were previously analysed by Raman spectroscopy and TPI. The dissolution test was performed for 24 h in a paddle dissolution apparatus according to USP (apparatus 2, Lambda 2 UV/Vis Spektrometer, Bodenseewerk Perkin–Elmer GmbH, Duesseldorf, Germany). In the case of the samples collected at the sampling points 0, 37 and 73 min full dissolution occurred already within 8 h as the coating thickness was not adequate to achieve sustained release, and the API was completely released after the coating was broken. Dissolution was carried out in 1 L deionised water as dissolution medium at 37 °C with a paddle rotation speed of 100 rpm. The drug concentration was determined online by UV spectroscopy (Lambda-2; Perkin–Elmer, Ueberlingen, Germany) during the dissolution testing. The spectrometer detection wavelength was set at 253 nm, corresponding to the maximum absorption of diprophylline in aqueous solution. Samples were measured in 3-min intervals. The resulting dissolution profiles were used to determine the mean

Table 1
Process parameters.

Step	Pan speed (rpm)	Spray rate (g/min)	Inlet air volume (m³/h)	Exhaust air temperature (°C)	Inlet air temperature (°C)
Warm up	5	–	120	45	55
Coating	22	6	150	38–43	50–55
Drying	22	–	150	50	50
Cooling	5	–	120	30	25

dissolution time (MDT). For the dissolution analysis six samples from each sampling interval were used.

2.6. Model development

Tablets collected at different stages of coating from batch A ($n = 42$) were used for offline quantitative calibration development. The coating thickness measured by TPI analysis and the MDT determined by the dissolution test were used as reference analytical methods.

For model validation samples were collected in the same way at each sampling point of batch B ($n = 36$) using the MDT as the reference analytical method.

The coating thickness (in µm) of the same tablets of batch A ($n = 42$) that were used to construct the PLS model with the MDT as reference analytical method (see chapter 3.2) were measured by TPI analysis from both sides. Afterwards the two measurements of the respective sample were averaged and were used for the model development. In addition an extra set of validation samples from batch A ($n = 12$) and batch B ($n = 12$) was collected at each sampling point for model validation.

2.7. In-line monitoring

A noncontact Raman probe was fixed outside the coating pan facing the tablet bed to collect spectra during the process. The working distance to the tablet bed was about 22 cm. To protect the probe against dust compressed air was blown through an iron pipe [95 mm length, 33 mm diameter], which was attached in front of the probe. For each spectrum the Raman signal was averaged for 15 s (whereby approx. 1250 tablets were moving through the measurement spot during this period) followed by cosmic ray filtering.

2.8. Multivariate data analysis

A multivariate model was constructed for batch A by correlating Raman spectral data with MDT (min) and coating thickness (µm) using PLS. The calibration model was based upon a set of 42 tablets for MDT or 36 tablets for coating thickness. To estimate the applicability of the constructed model it was tested on an independent batch (batch B). The samples were collected and analysed as described in chapters 2.2 and 2.3.

The PLS model and data pre-processing (mean centring and SNV) was carried out using the Simca-P + software (version 11.5, Umetrics AB, Umeå, Sweden). Additionally, multivariate curve resolution (MCR) was performed using the HoloREACT™ (Kaiser Optical Systems) reaction analysis software.

3. Results and discussion

3.1. Spectral analysis

For the model development the region from 1550 to 1810 cm^{-1} was used. In Fig. 1 baseline-corrected Raman spectra of tablets at different stages of the coating process are plotted. The spectra demonstrate the sensitivity of the Raman signal to changes in the coating level on tablets. The intensity of the peaks 1604, 1646 and 1690 cm^{-1} (Fig. 1, points 1–3) decreased as function of coating time, and these spectral features can all be assigned to diprophylline. In contrast the intensity of the peak at 1734 cm^{-1} increased as a function of coating time. This vibrational mode can be assigned to the carbonyl group of the polyvinyl acetate (Fig. 1, point 4). The MCR results (Fig. 2) of the calibration data set (batch A; $n = 42$) show that the same trend for the Raman spectra with coating time can be obtained using a two-factorial model.
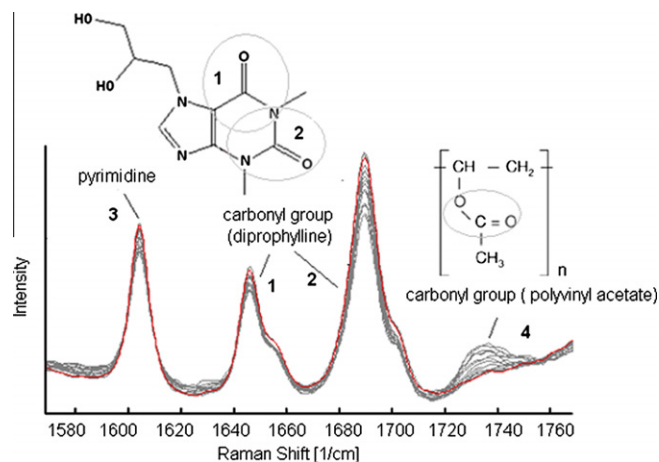

Fig. 1. Baseline corrected spectra of tablets during the coating process. (For interpretation of the references to colour in this figure legend, the reader is referred to the web version of this article.)
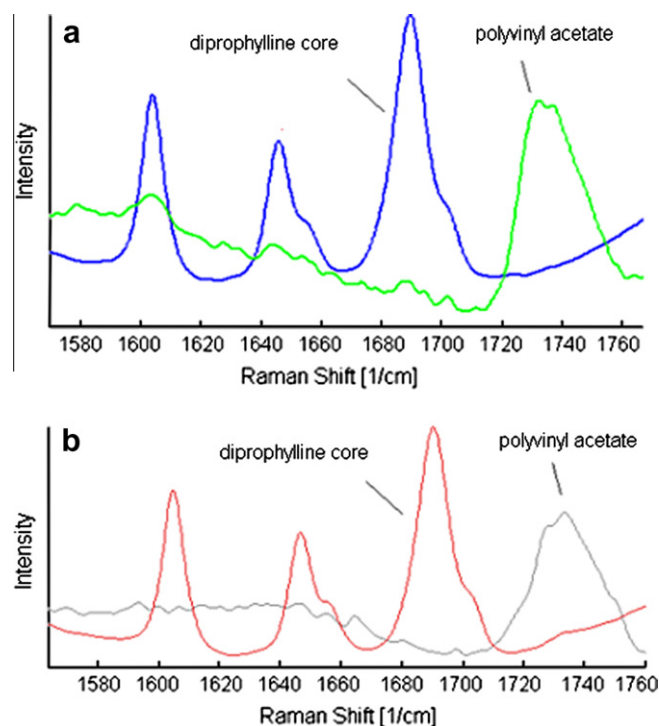

Fig. 2. Reproduced spectra by MCR of coating material and diprophylline core (a) compared to the Raman spectra (b). (For interpretation of the references to colour in this figure legend, the reader is referred to the web version of this article.)

Fig. 2 shows the resultant basis spectra of the two components. The reproduced spectra were similar to the spectra of the diprophylline core and the coating material. The score values of the components (Fig. 3) show that the contribution of the core to the analytical signal decreased and that the contribution of the coating to the signal increased with coating time. As expected from the Raman spectra (Fig. 1) the contribution of the coating material to the Raman signal is marginal compared to the core signal.

3.2. Mean dissolution time (MDT)

Fig. 4 shows the dissolution profile for coated samples collected at 73 min coating time (a) and at the end of the process (b). In the
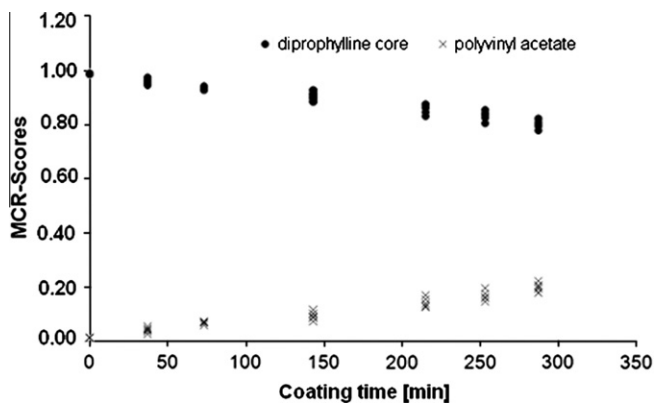
Fig. 3. MCR scores (batch A; $n = 42$) as a function of coating time.

case of the finished coated tablets (b) the dissolution profile followed a zero order kinetics after a short delay, which was caused by the swelling of the film. Furthermore, the dissolution profile was reproducible. At 73 min coating time (a) the dissolution profile of the investigated samples showed a high variability. Fig. 4a shows that the dissolution profile of the coated tablets changed after 50–150 min. The sudden increase in released active ingredient indicates that the film had burst due to its low coating thickness and, thus, the active ingredient was completely released. In the initial phase of the coating process the coating layer is inhomogeneous, which explains the variation in time points for the bursting of the film and thus the high variability in MDT values. Table 2 shows the calculated MDT values at different sampling points in time for batch A and B. The inhomogeneity in the coat resulted in a high variability of the MDT, which complicated the model development. While it was possible to estimate the overall amount of coating per tablet using Raman spectroscopy, it was not possible to detect the inter- and intra-coating inhomogeneity, which led to a variation in the burst and the MDT. This is due to the large spot size used in the Raman measurement. Table 2 shows by means of the coefficient of variation that the variation of the MDT decreased after 148 min coating time. This indicates that after 148 min coating time the film thickness is adequate and provides an intact coat over the dissolution period. From this time point on, it is possible to link the MDT to the coating amount.

3.3. PLS model

A PLS predictive model with four principal components was constructed using the SNV spectral data obtained by tablets

collected at different stages of coating from batch A ($n = 42$). The root mean square error of calibration (RMSEC) was 23.7 min for the tablet set of 15.7–359.2 min MDT ($n = 42$). The validation set ($n = 36$) of the independent batch B resulted in a root means square errors of prediction (RMSEP) of 36.6 min ($n = 36$; 48–353 min MDT).

Fig. 5 shows the predicted MDT resulting from the in-line measured spectra (batch A and B) against coating time together with the dissolution results from the samples that were collected for off-line analysis during the process (Table 2).

As discussed, after 148 min coating time the film thickness is adequate and provides an intact coat throughout the dissolution period. From 148 min coating time onwards the MDT predicted from the in-line data using the PLS model is in good agreement with the offline measured samples that were collected during the coating process.

3.4. Terahertz pulsed imaging (TPI)

Using TPI it is possible to map the coating thickness distribution over the entire surface of the tablet in order to determine the intra-tablet coating homogeneity and to detect coating ruptures.

As an example the results of the TPI measurements of two tablets at coating times of 287 min and 73 min are shown in Fig. 6. In the case of the layer thickness maps (Fig. 6a and b) every pixel is colour coded according to its coating thickness. The information from the coating maps can also be represented in a histogram (Fig. 6c and d).

Table 3 shows the coating thickness as measured by TPI with coating time. The 95% confidence interval (CI) shows that the coating thicknesses of the tablets after coating times of 37 min and 73 min are not significantly different. From 73 min onwards the coefficient of variation decreased noticeably, indicating an improved coating homogeneity. As outlined above before 148 min process time the coating thickness is not adequate in order to provide a stable coating during dissolution (see Section 3.2). No strong difference with regard to the coating thickness was found between the tablets sampled after 258 min and 287 min coating time. However, similar to the observation at the beginning of the coating process the coefficient of variation decreased noticeably during this period, indicating an improved coating homogeneity at the end of the coating process.

A multivariate model was constructed by correlating the coating thickness (μm) obtained by the tablets of batch A ($n = 42$; 0–145.9 μm) with pre-processed Raman spectral data in the region 1550–1810 cm^{-1} using PLS. Fig. 7 shows the loading plot (a) and
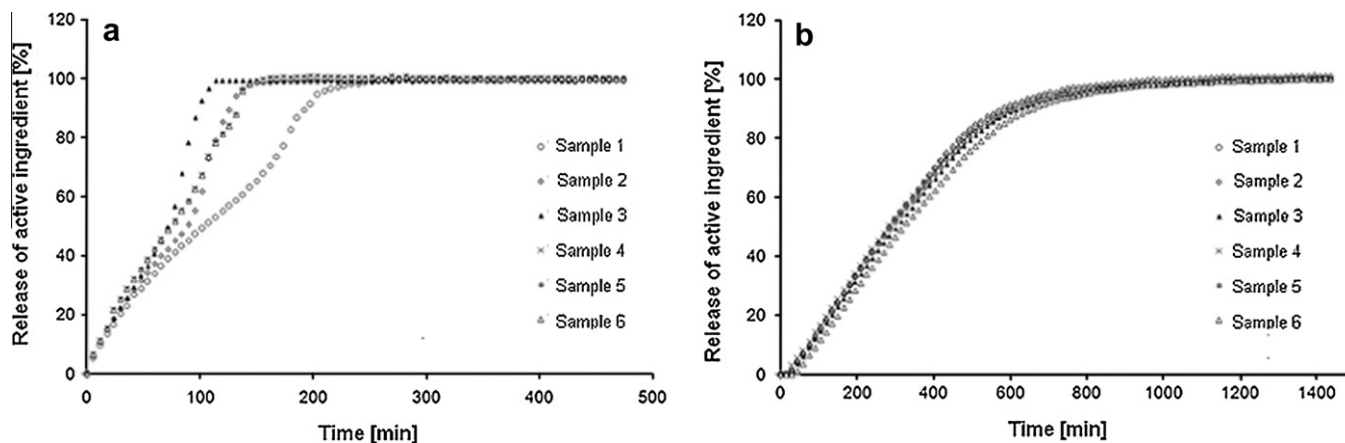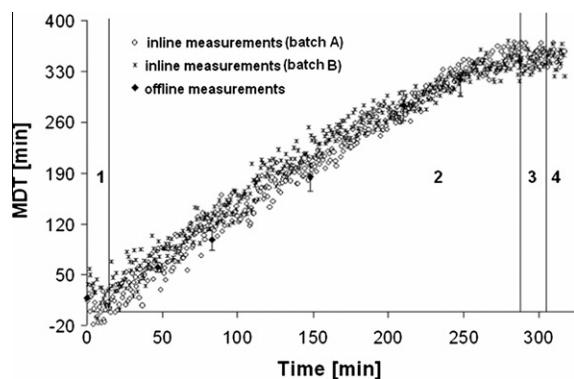

Fig. 4. Dissolution profile of samples collected after 73 min coating time (a) and at the end of the process (b).

Table 2
Calculated MDT of the samples (batch A and B; $n = 12$) collected at different coating times.

Theoretical polymer amount (mg/cm^2)	Coating time (min)	MDT			
		Mean (min)	SD (min)	CV (%)	95% CI
0	0	17.3	1.6	9.4	0.9
1	37	60.0	13.4	22.3	7.3
2	73	97.7	25.9	26.5	14.1
4	148	184	35.8	19.4	19.5
6	220	283	37.2	13.1	20.2
7	258	319	42.5	13.4	23.1
8	287	345	20.3	5.9	11.1

Table 3
Coating thickness of the samples measured by TPI (batch A; $n = 6$) collected at different coating times.

Theoretical polymer amount (mg/cm^2)	Coating time (min)	Coating thickness (µm)			
		Mean (µm)	SD (µm)	CV (%)	95% CI
1	37	45.5	5.6	12.2	4.4
2	73	51.4	3.8	7.4	3.0
4	148	77.0	4.8	6.2	3.8
6	220	105	7.0	6.6	5.6
7	258	124	8.9	7.2	7.1
8	287	136	5.3	3.9	4.2

Fig. 5. Prediction of MDT for trials A and B from in-line data ($n = 12$; mean ± CI 95%); process steps: 1, warm up; 2, coating; 3, drying; and 4, cooling.

the score plot (b) of the first principal component. The loading plot shows the three characteristic peaks of the diprophylline and the peak of the carbonyl group of the polyvinyl acetate (Fig. 1). Unlike the Raman spectrum the loading plot shows negative peaks at the same wavenumbers as the Raman spectral features indicating the

attenuation of the Raman signal in dependence on the coating thickness. Fig. 7b presents the score plot ($u1 \times t1$) of the first principal component. In general these plots display the observations in the projected X (T) and Y (U) space, and show how well the Y space (coating thickness) correlates with the X space (Raman spectra) [36]. It is noticeable that the variances in the Raman spectra in dependence on the coating time are not in a linear relation with the coating thickness but could be better described using a quadratic function. By investigating the skewness value of the x-variables an average value of about −1.2 is determined, which corresponds to a distribution with a tail to the left. One way to achieve approximate normality is by means of variable transformation. After performing the square root transformation of the x-variables, a near-zero value of skewness (<0.3) was achieved indicating a symmetrical data distribution. Furthermore, the score plot ($u1 \times t1$) (Fig. 8) shows an approximate linear correlation between the variance of the x- and y-variables after the transformation. Consequently, the model development was performed with the transformed Raman spectra.

The uncoated diprophylline tablets were excluded from the model development. By means of the software Simca it is possible to detect outliers with the "Distance to model (DMod)" function. It computes the observation distance to the model in the X space (DModX) and in the Y space (DModY). Depending on the selected
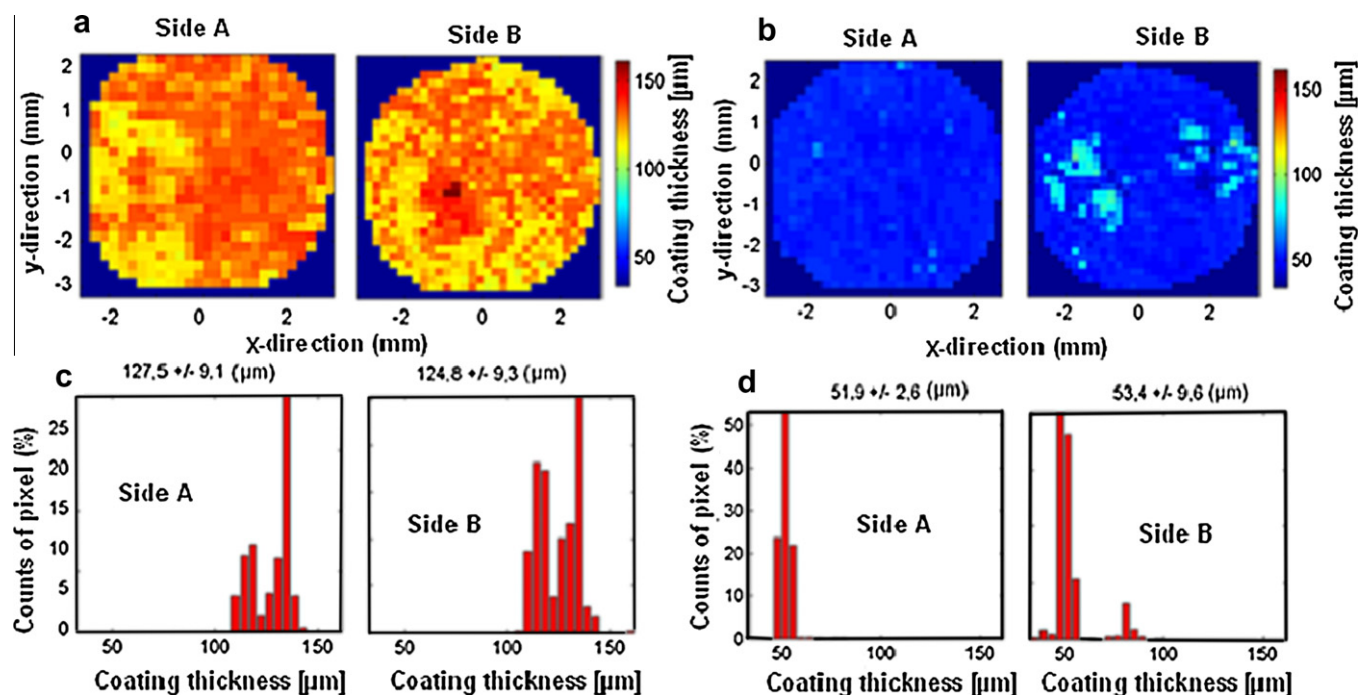
Fig. 6. Layer thickness maps (a and b) and histograms of the coating thickness distribution (c and d) for tablets after a coating time of 287 min (a and c) and 73 min (b and d).
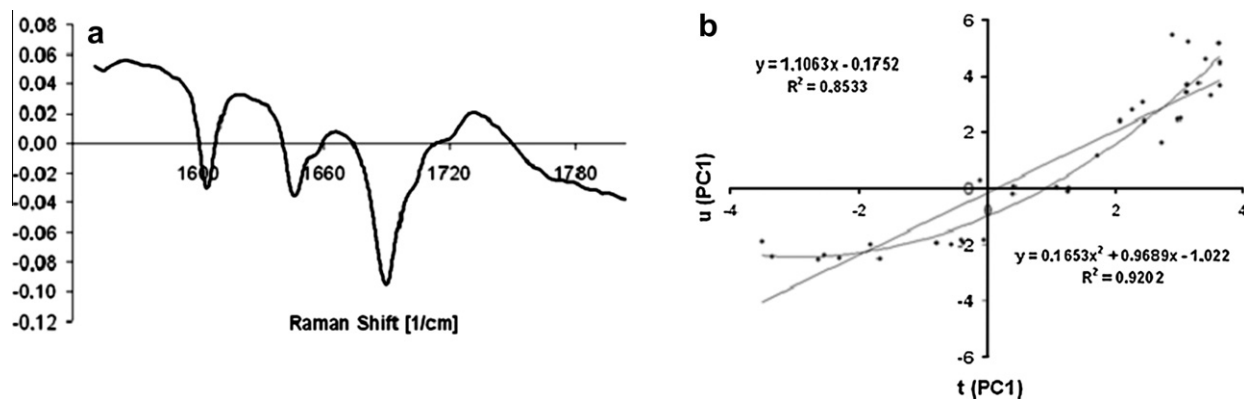
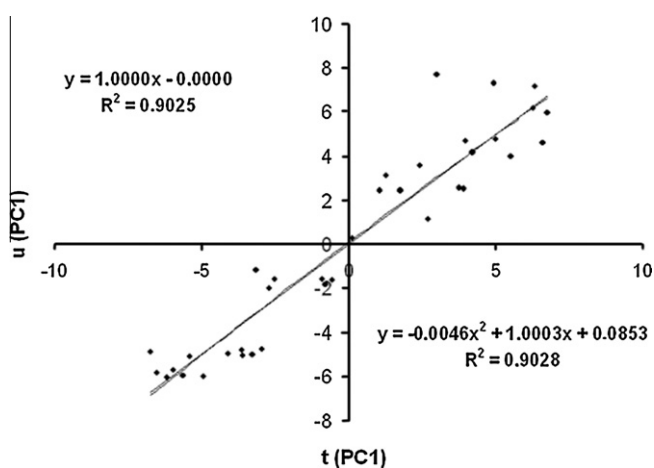Fig. 7. Loading plot (a) and score plot (b) of the first principal component.

Fig. 8. Score plot of the first principal component after square root transformation.

significance level ($\alpha = 0.05$) the critical distance to the model for observations in the workset is computed. Observations outside the critical distance are defined as outliers. Detailed information on the calculation and estimation process is described in the literature [35]. The DModX plot shows that the uncoated diprophylline tablets are outside the critical distance and are not linked to the explanation of the variance of the Raman spectra (x variables) by the principal components (Figure not shown). This can be explained by the subtle contribution of the coating material to the Raman signal compared to the strong contribution from the core signal (see Section 3.1). During the whole process the core signal dominates the Raman signal and even at the process end point the contribution of the coating material to the Raman signal is only marginal. Consequently, there is no distinct difference between the Raman signal of the uncoated and 37 min coated tablets, and it is thus not possible to distinguish between the two sets of tablets. However, a coating thickness of 45 μm is achieved after 37 min, which represents one-third of the total coating thickness at the end of the process (136 μm) which is not equal to the variance in the Raman spectra. Thus, the uncoated tablets are not linked to the explanation of the variance of the Raman spectra (x variables) by the principal components and are excluded from the workset. Consequently, it is not possible to monitor the beginning of the process by in-line Raman measurements and an adequate coating amount is necessary in order to predict the coating thickness.

Finally, a multivariate model was constructed by correlating the coating thickness (μm) as measured by TPI obtained by the tablets of batch A ($n = 36$) with pre-processed, transformed Raman spectral data in the region 1550–1810 cm^{-1} using PLS. The RMSEC was
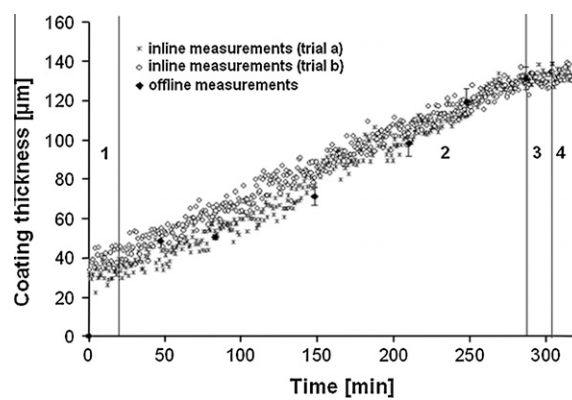

Fig. 9. Predicted coating thickness (μm) for trials A and B from in-line data ($n = 10$; mean ± CI 95%); process steps: 1, warm up; 2, coating; 3, drying; and 4, cooling.

6.5 μm for the tablet set of 43.2–145.9 μm ($n = 36$). The first validation set ($n = 12$; batch A; 44.4 μm to 123.8 μm) and the second validation set of the independent batch B ($n = 12$; 49.6 μm to 138.2 μm) resulted in a RMSEP of 17.1 μm and 16.8 μm, respectively.

Fig. 9 shows the predicted coating thickness resulting from the in-line measured spectra (batch A and B) with coating time compared to the offline measured samples ($n = 10$) that were collected at the corresponding sampling points.

The coating thickness predicted by the in-line data agrees well with the measured samples that were collected for offline analysis. However, as discussed before it was not possible to monitor the beginning of the process because a thickness below 30–40 μm cannot be determined precisely by TPI.

3.5. Comparison of the two reference analysis techniques dissolution test and TPI

Fig. 10 illustrates the reference values that were determined for batch A with coating time. As discussed in Section 3.3 the correlation between coating thickness (Fig. 10b) and coating time was better described by a quadratic function compared to the MDT (Fig. 10a). Furthermore, it is noticeable that the MDT as determined by dissolution testing and coating thickness of the respective coated tablet are not linearly correlated (Fig. 11). Thus, two different models for the respective reference analytical method were developed. By using both reference values (MDT, coating thickness) together for the model development, an agreement is necessary in order to find a functional correlation between the variance in the Raman spectra and the two reference values. This results in an
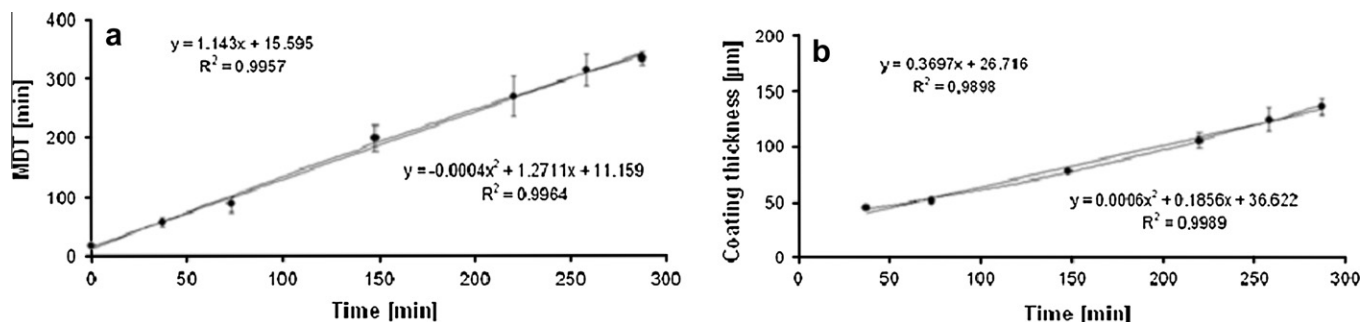
Fig. 10. MDT (a) and coating thickness (b) with coating time of batch A ($n = 6$; mean ± CI 95%).
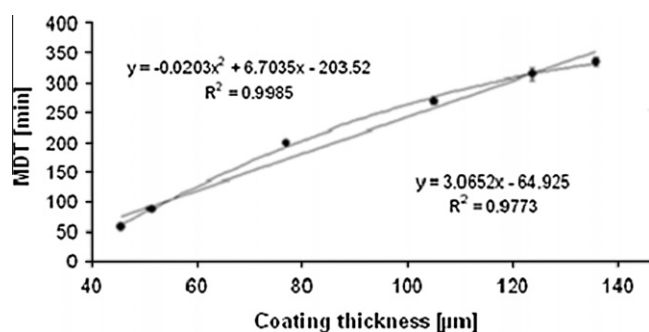

Fig. 11. MDT vs. coating thickness (batch A; mean; $n = 6$, 37–287 min).

inappropriate model with lower predictive power compared to the models that were developed with only one of the reference values.

As discussed in Section 3.2 after 148 min coating time the film thickness is adequate and provides an intact coating over the dissolution period. Consequently, from this time point onwards, there is a linear relation between the MDT and the coating thickness because the MDT is linked to the amount of coating.

4. Conclusion

It was possible to implement Raman spectroscopy as a non-invasive and rapid PAT tool for quantitative in-line monitoring of functional coating by correlating the Raman spectra with the MDT and coating thickness. Both reference techniques require a minimum amount of coating, which leads to complications to monitor the beginning of the process when the coating thickness cannot be resolved by either spectroscopic technique.

Furthermore, there is no linear correlation between the MDT and coating thickness of the respective coated tablets. Thus, two different models with the respective reference analytical method were necessary in order to achieve a high efficiency in data analysis.

On the basis of Raman spectra acquired using the in-line probe, it was possible to estimate the coating thickness during the coating process. However, it was not possible to measure the inter- and intra-coating inhomogeneity during the in-line measurements due to the large spot size and the long averaging time of the measurement. We found that the inter- and intra-coating inhomogeneity dominated the drug release characteristics until a sufficiently thick coating barrier was established after 148 min coating time. It was not possible to predict the MDT with an adequate accuracy in the beginning of the process.

Using in-line Raman measurements it was possible to detect the end point of the process, where the required amount of coating was present in order to achieve the desired MDT or coating thickness.

References

[1] Z.J. Shao, L. Morales, S. Diaz, N.A. Muhammad, Drug release from Kollicoat SR 30D-coated nonpareil beads: evaluation of coating level, plasticizer type, and curing conditions, AAPS PharmSciTech 3 (2002) 1–10.
[2] United States Pharmacopeia, US Pharmacopeial Convention Inc., Rockville, 2008.
[3] F. Li-Fang, H. Wei, C. Yong-Zhen, X. Bai, D. Xing, W. Feng, Q. Min, C. De-Ying, Studies of chitosan/Kollicoat SR 30D film-coated tablets for colonic drug delivery, International Journal of Pharmaceutics 375 (2009) 8–15.
[4] K.R. Be, W.W. Blaser, R.A. Bredeweg, J.P. Chauvel Jr., R.S. Harner, M. LaPack, A. Leugers, D.P. Martin, L.G. Wright, E.D. Yalvac, Process analytical chemistry, Analytical Chemistry 65 (1993) 199R–216R.
[5] J. Tenhunen, K. Sjöholm, K. Pietilä, S. Home, Determination of fermentable sugars and nitrogenous compounds in wort by near- and mid-infrared spectroscopy, Journal of the Institute of Brewing and Distilling 100 (1994) 11–15.
[6] J. Workman Jr., M. Koch, D. Veltkamp, Process analytical chemistry, Analytical chemistry 79 (2007) 4345–4364.
[7] Food and Drug Administration (FDA), Guidance for Industry: PAT – A Framework for Innovative Pharmaceutical Development, Manufacturing and Quality Assurance, 2004. <www.fda.gov/downloads/Drugs/GuidanceComplianceRegulatoryInformation/Guidances/UCM070305.pdf>.
[8] J. Rantanen, Process analytical application of Raman spectroscopy, Journal of Pharmacy and Pharmacology 59 (2007) 171–177.
[9] K.R. Morris, S.L. Nail, G.E. Peck, S.R. Byrn, U.J. Griesser, J.G. Stowell, S.-J. Hwang, K. Park, Advances in pharmaceutical materials and processing, Pharmaceutical Science and Technology Today 1 (1998) 235–245.
[10] G. Dünnebier, H. Tups, FDA PAT Initiative – Eine Anwendersicht zu technischen Möglichkeiten und aktueller industrieller Umsetzungen, Chemie Ingenieur Technik 79 (2007) 2019–2028.
[11] B.R. Buchanan, M.A. Baxter, T.-S. Chen, X.-Z. Qin, P.A. Robinson, Use of near-infrared spectroscopy to evaluate an active in a film coated tablet, Pharmaceutical Research 13 (1996) 616–621.
[12] A.S. El-Hagrasy, F. D'Amico, J.K. Drennen III, A process analytical technology approach to near-infrared process control of pharmaceutical powder blending. Part I: D-optimal design for characterization of powder mixing and preliminary spectral data evaluation, Journal of Pharmaceutical Sciences 95 (2006) 392–406.
[13] A.S. El-Hagrasy, M. Delgado-Lopez, J.K. Drennen III, A process analytical technology approach to near-infrared process control of pharmaceutical powder blending. Part II: Qualitative near-infrared models for prediction of blend homogeneity, Journal of Pharmaceutical Sciences 95 (2006) 407–421.
[14] A.S. El-Hagrasy, J.K. Drennen III, A process analytical technology approach to near-infrared process control of pharmaceutical powder blending. Part III: Quantitative near-infrared calibration for prediction of blend homogeneity and characterization of powder mixing kinetics, Journal of Pharmaceutical Sciences 95 (2006) 422–434.
[15] A.S. El-Hagrasy, S.Y. Chang, S. Kiang, Evaluation of risk and benefit in the implementation of near-infrared spectroscopy for monitoring of lubricant mixing, Pharmaceutical Development and Technology 11 (2006) 303–312.
[16] M. Andersson, S. Folestad, J. Gottfries, M.O. Johansson, M. Josefson, K.-G. Wahlund, Quantitative analysis of film coating in a fluidized bed process by in-line NIR spectrometry and multivariate batch calibration, Analytical Chemistry 72 (2000) 2099–2108.
[17] M. Andersson, M. Josefson, F.W. Langkilde, K.-G. Wahlund, Monitoring of a film coating process for tablets using near infrared reflectance spectrometry, Journal of Pharmaceutical and Biomedical Analysis 20 (1999) 27–37.
[18] J.D. Kirsch, J.K. Drennen, Determination of film-coated tablet parameters by near-infrared spectroscopy, Journal of Pharmaceutical and Biomedical Analysis 13 (1995) 1273–1281.
[19] T.R. De Beer, W.R. Baeyens, J. Ouyang, C. Vervaet, J.P. Remon, Raman spectroscopy as a process analytical technology tool for the understanding and the quantitative in-line monitoring of the homogenization process of a pharmaceutical suspension, Analyst 131 (2006) 1137–1144.
[20] T.R.M. De Beer, P. Vercruysse, A. Burggraeve, T. Quinten, J. Ouyang, X. Zhang, C. Vervaet, J.P. Remon, W.R.G. Baeyens, In-line and real-time process monitoring

of freeze drying process using Raman and NIR spectroscopy as complementary process analytical technology (PAT) tools, Journal of Pharmaceutical Sciences 98 (2009) 3430–3445.

[21] T.R.M. De Beer, C. Bodson, B. Dejaegher, B. Walczak, P. Vercruysse, A. Burggraeve, A. Lemos, L. Delattre, Y. Vander Heyden, J.P. Remon, C. Vervaet, W.R.G. Baeyens, Raman spectroscopy as a process analytical technology (PAT) tool for the in-line monitoring and understanding of a powder blending process, Journal of Pharmaceutical and Biomedical Analysis 48 (2008) 772–779.

[22] G.J. Vergote, T.R. De Beer, C. Vervaet, J.P. Remon, W.R. Baeyens, N. Diericx, F. Verpoort, In-line monitoring of a pharmaceutical blending process using FT-Raman spectroscopy, European Journal of Pharmaceutical Sciences 21 (2004) 479–485.

[23] S. Romero-Torres, J.D. Perez-Ramos, K.R. Morris, E.R. Grant, Raman spectroscopic measurement of tablet-to-tablet coating variability, Journal of Pharmaceutical and Biomedical Analysis 38 (2005) 270–274.

[24] S. Romero-Torres, J.D. Perez-Ramos, K.R. Morris, E.R. Grant, Raman spectroscopy for tablet coating thickness quantification and coating characterization in the presence of strong fluorescent interference, Journal of Pharmaceutical and Biomedical Analysis 41 (2006) 811–819.

[25] A.S. El-Hagrasy, S.-Y. Chang, D. Desai, S. Kiang, Application of Raman spectroscopy for quantitative in-line monitoring of tablet coating, American Pharmaceutical Review 9 (2006) 40–45.

[26] A.S. El-Hagrasy, S.-Y. Chang, D. Desai, S. Kiang, Raman spectroscopy for the determination of coating uniformity of tablets: assessment of product quality and coating pan mixing efficiency during scale-up, Journal of Pharmaceutical Innovation 1 (2006) 37–42.

[27] J. Müller, K. Knop, J. Thies, C. Uerpmann, P. Kleinebudde, Feasibility of Raman spectroscopy as PAT tool in active coating, Drug Development and Industrial Pharmacy 36 (2010) 234–243.

[28] L. Maurer, H. Leuenberger, Terahertz pulsed imaging and near infrared imaging to monitor the coating process of pharmaceutical tablets, International Journal of Pharmaceutics 370 (2009) 8–16.

[29] L. Ho, R. Müller, K.C. Gordon, P. Kleinebudde, M. Pepper, T. Rades, Y. Shen, P.F. Taday, J.A. Zeitler, Monitoring the film coating unit operation and predicting drug dissolution using terahertz pulsed imaging, Journal of Pharmaceutical Sciences 98 (2009) 4866–4876.

[30] L. Ho, R. Müller, M. Römer, K.C. Gordon, J. Heinämäki, P. Kleinebudde, M. Pepper, T. Rades, Y. Shen, C.J. Strachan, P.F. Taday, J.A. Zeitler, Analysis of sustained-release tablet film coats using terahertz pulsed imaging, Journal of Controlled Release 119 (2007) 253–261.

[31] J.A. Zeitler, Y. Shen, C. Baker, P.F. Taday, M. Pepper, T. Rades, Analysis of coating structures and interfaces in solid oral dosage forms by three dimensional terahertz pulsed imaging, Journal of Pharmaceutical Sciences 96 (2007) 330–340.

[32] B. Skalsky, T. Felisiak, H.-U. Petereit, Eudragit – application Guidelines, Evonik Röhm GmbH, Darmstadt, 2009.

[33] K.H. Bauer, K. Lehmann, H.P. Osterwald, G. Rothgang, Überzogene Arzneiformen, Wissenschaftliche Verlagsgesellschaft mbH, Stuttgart, 1988.

[34] J. Kim, J. Noh, H. Chung, Y.-A. Woo, M.S. Kemper, Y. Lee, Direct, non-destructive quantitative measurement of an active pharmaceutical ingredient in an intact capsule formulation using Raman spectroscopy, Analytica Chimica Acta 598 (2007) 280–285.

[35] M. Kim, H. Chung, Y. Woo, M. Kemper, New reliable Raman collection system using the wide area illumination (WAI) scheme combined with the synchronous intensity correction standard for the analysis of pharmaceutical tablets, Analytica Chimica Acta 579 (2006) 209–216.

[36] L. Eriksson, E. Johansson, N. Kettaneh-Wold, J. Trygg, C. Wikström, S. Wold, Multi- and megavariate data analysis. Part I: Basic principles and applications, Umetrics, Umea, 2006.